applied optics

Spatially resolved photodiode response for simulating precise interferometers

Germán Fernández Barranco,[1,2,*] Michael Tröbs,[1,2] Vitali Müller,[1,2] Oliver Gerberding,[1,2] Frank Seifert,[1,3] and Gerhard Heinzel[1,2]

[1]Max Planck Institute for Gravitational Physics (Albert Einstein Institute), Callinstrasse 38, 30167 Hannover, Germany
[2]Institut für Gravitationsphysik, Leibniz Universität Hannover, Callinstrasse 38, 30167 Hannover, Germany
[3]Present address: National Institute of Standards and Technology, 100 Bureau Dr., Gaithersburg, Maryland 20899, USA
*Corresponding author: German.Fernandez. Barranco@aei.mpg.de

Received 24 May 2016; revised 30 July 2016; accepted 30 July 2016; posted 2 August 2016 (Doc. ID 266862); published 17 August 2016

Quadrant photodiodes (QPDs) are used in laser interferometry systems to simultaneously detect longitudinal displacement of test masses and angular misalignment between the two interfering beams. The latter is achieved by means of the differential wavefront sensing (DWS) technique, which provides ultra-high precision for measuring angular displacements. We have developed a setup to obtain the spatially resolved response of QPDs that, together with an extension of the simulation software IfoCAD, allows us to use the measured response in simulations and accurately predict the desired longitudinal and DWS phase observables. Three different commercial off-the-shelf QPD candidates for space-based interferometry were characterized. The measured response of one QPD was used in optical simulations. Nonuniformities in the response of the device and crosstalk between segments do not introduce significant variations in the longitudinal and DWS measurands with respect to the standard case when a uniform QPD without crosstalk is used.

OCIS codes: (120.0120) Instrumentation, measurement, and metrology; (120.3180) Interferometry; (120.4640) Optical instruments; (150.5495) Process monitoring and control; (230.5170) Photodiodes.

http://dx.doi.org/10.1364/AO.55.006688

1. INTRODUCTION

Laser interferometry for intersatellite ranging is the key technology for eLISA, the future space-based gravitational wave detector. It is also expected to improve the sensitivity of the GRACE Follow-On (GRACE-FO) mission, which is planned to continue gravity-field measurements like the previous GRACE mission. In the type of interferometer used in these missions, the main longitudinal signal is proportional to the quadrant photodiode (QPD) mean phase when the electric field intensities of the two interfered beams are integrated over its surface [1]. Additionally, the angle between these beams is measured using the differential wavefront sensing (DWS) technique [1–3], which relies on the differential phase. QPDs used in our models have a uniform profile with no crosstalk between adjacent segments. We call them standard QPDs. Real QPDs might feature a nonuniform spatial response and crosstalk between adjacent segments. Nonuniformities could originate from dust particles or contamination on the QPD surface, misplaced wires, manufacturing defects, or the internal structure of the QPD. Visual inspection (i.e., with a microscope) helps in identifying some of these issues, but does not produce any quantitative information about their influence on the phase readout that could affect the longitudinal and DWS measurands mentioned above.

There has been research on the spatial response of photodetectors at different wavelengths [4–13]. In this work, we measure the spatially resolved responses of QPDs and use the measured data to simulate interferometer signals in laser interferometers. We describe the development of a computer-aided control-and-acquisition setup to obtain spatially resolved responses of QPDs at a wavelength close to 1064 nm. Additionally, we have extended our optical simulation toolbox IfoCAD [14] to include the measured QPD responses in simulations. This allows us to study for the first time to the best of our knowledge the effect of real QPD features, such as nonuniformities and crosstalk, on the measurands of the interferometric system and thus close an important gap in the modeling of precise interferometers.

In Section 2, we present the setup built for the spatial characterization of QPDs. Section 3 shows the measured spatial response of three QPD candidates for space-based interferometry. In Section 4, the optical simulation toolbox IfoCAD and its extension to include measured QPD responses are introduced. A description of the simulation environment used and results obtained with the standard QPD and the measured QP22 can

be found in Section 5. Finally, conclusions from the results and the outlook for the setup and simulations are discussed in Section 6.

2. SPATIAL CHARACTERIZATION SETUP

Figure 1 shows the schematic of the setup where the light of a fiber-pigtailed laser diode with a 1066.7 nm center wavelength (LPS-1060-FC by Thorlabs) is collimated and injected onto a small optical bench. A lens with 50 mm focal length is used to focus the beam onto the device under test (DUT). A beam diameter of 50 μm at the DUT was used in this work. The DUT is connected to a four-channel transimpedance amplifier (TIA). The DUT can be scanned laterally over a 50 mm × 50 mm area by means of stacked translation stages. The distance between the DUT and beam waist in the z axis is controlled by a third translation stage (M-405.CG by Physik Instrumente).

The motion of the translation stages, as well as the sampling of the TIA output, is controlled by a LabVIEW program. The PCI-6014 DAQ card by National Instruments used in the setup samples the four channels at 200 kS/s with 16-bit resolution.

The optimal focusing of the laser beam on the DUT is achieved with the following procedure: The knife-edge method [15] is used to determine the beam diameter and is repeated for a number of z positions. The beam diameter of a Gaussian beam as a function of propagation distance is fitted to the measured diameter-distance pairs. The final z position is chosen at the location of the fitted waist.

Once the focusing of the beam on the DUT is done, the spatial response scan is performed with a translation in the x axis where the photodiode moves from a starting point x_0 to a final point x_f, while the acquisition system records the QPD output signals using a sampling rate (f_s) that can be modified in every scan. Increasing f_s directly results in an increase of the number of samples in the x coordinate $(x_0, x_1, x_2, \ldots, x_f)$. Choosing an f_s that generates x-axis steps ($\Delta x = x_{i+1} - x_i$) very much below the laser spot size does not increase the resolution further since the detection of changes in the photodiode response is ultimately limited by the beam diameter. Additionally, only samples obtained when moving at constant velocity are stored in this part, while those recorded during the acceleration and deceleration phases of the translation stage are discarded. After the data have been recorded, the DUT returns to its start position x_0 and increments the y position. Recording data only in one direction of the x axis was chosen to eliminate the effects of hysteresis and mechanical play in the translation stage. This procedure is repeated several times within a y-axis range specified by the starting and final point (y_0, y_f) and the step size (Δy). Typical step sizes in x and y are below 10 μm.

3. MEASURED SPATIAL RESPONSE OF QPD CANDIDATES

Figure 2 presents the normalized spatially resolved response of the QP22 by First Sensor, a ∼5-mm-diameter silicon QPD. The single segment response shows crosstalk between adjacent segments (see Case 4 in Fig. 8), which is discussed in Section 5 below. The sum of the four QPD segments was used for Fig. 2. The measurement shows spots across the photodiode surface with a 20% reduced responsivity. The spots are distributed in columns 0.4 mm apart. The distance between two consecutive spots within a column is also 0.4 mm. The QP22 is a silicon-based device designed to work at a wavelength of 1064 nm. The low absorption of silicon in this wavelength range (typical responsivity of 0.2 A/W) is compensated by using a diffusely reflective layer below the active material to achieve a responsivity of 0.5 A/W. The reflectivity of this additional layer is affected by internal connections of the photodiode at the observed spots, reducing the responsivity [16].

Figure 3 shows the normalized spatially resolved response of the GAP9119 by OEC GmbH, a 1-mm-diameter InGaAs QPD with a gap of 20 μm between the active areas. At the outer edge of each segment, an area with reduced responsivity and bonding wires is visible. Figure 4 shows the normalized response of the FCIQ1000 by OSI Optoelectronics, also a 1-mm-diameter InGaAs QPD but with a gap of 70 μm between the active areas. In both cases, the sum of the four

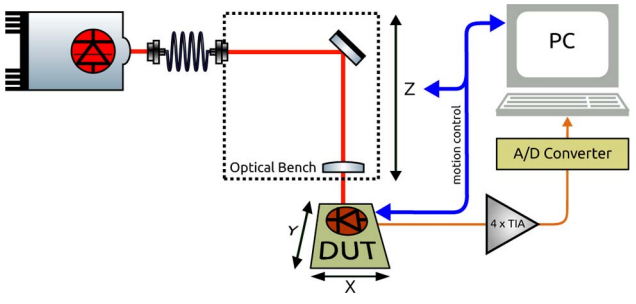

Fig. 1. Schematic description of the experimental setup to measure the spatial response of photodiodes. The light of a fiber-pigtailed laser diode is collimated and injected onto a small optical bench. A focusing lens is used to focus the beam onto the device under test (DUT). The DUT is connected to a four-channel transimpedance amplifier (TIA). The DUT position in the horizontal plane and the vertical position of the optical bench are set by translation stages. Motion of the stages and data sampling are controlled by a PC.

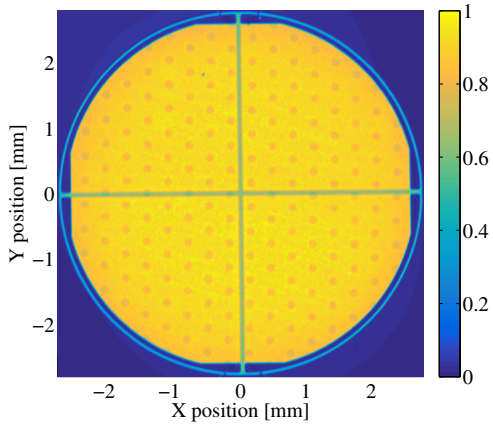

Fig. 2. Normalized spatially resolved response of the QP22 by First Sensor. The sum of the four QPD segments was used for the plot. The measurement shows a distribution of spots across the photodiode surface with a 20% reduced responsivity.

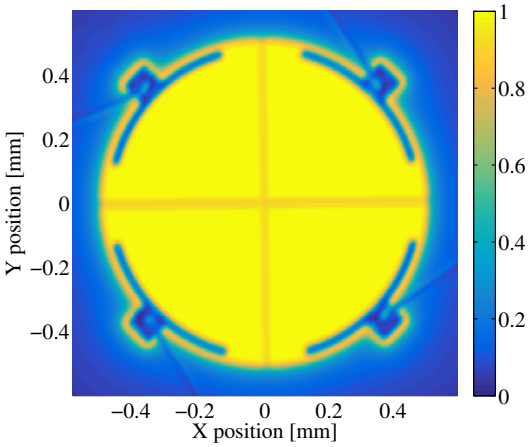

Fig. 3. Normalized spatially resolved response of the GAP9119 by OEC GmbH. The sum of the four QPD segments was used for the plot. The responsivity deviation within the active area is around 1%.

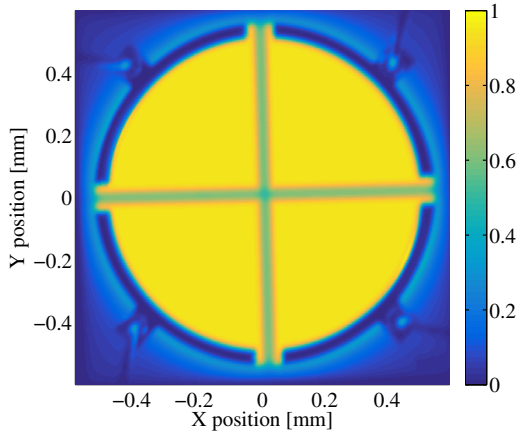

Fig. 4. Normalized spatially resolved response of the FCIQ1000 by OSI Optoelectronics. The sum of the four QPD segments was used for the plot. The responsivity deviation within the active area is around 1%.

QPD segments was used for the plots, and the responsivity deviation within the active area is around 1%.

4. IFOCAD TOOLBOX

IfoCAD is a C/C++ software developed at the Albert Einstein Institute in Hannover to simulate and optimize laser interferometers. IfoCAD can compute heterodyne signals as present in longitudinal path length, DWS, differential power sensing (DPS), and contrast measurements [14]. At the core of IfoCAD, the electric fields of two interfering beams are integrated over the photodiode surface. So far, the response of the photodiode was assumed to be uniform over a given segment and zero outside. With the extension developed here, a certain photodiode response can be used to substitute the standard IfoCAD photodiode. Four matrices, describing the response of each segment, are loaded into the program during the simulation. The integration of the electric fields is performed as described in expression (1)

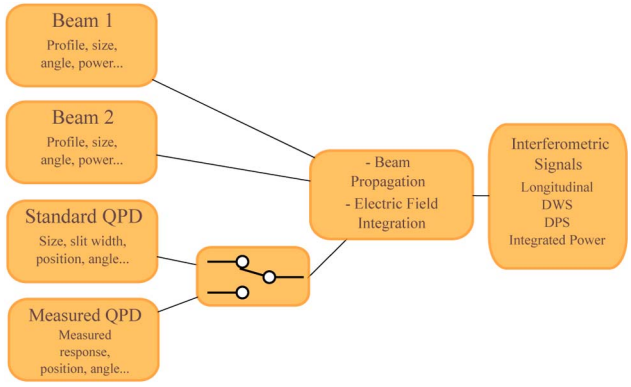

Fig. 5. Flowchart of an IfoCAD simulation including the extension for measured QPD responses. First, the two interfering beams and the QPD are created and their parameters specified. At this stage, we can choose between the standard QPD model or a measured QPD response. Then, IfoCAD propagates the beams until they reach the QPD position and integrates the electric fields over the given surface. After that, the main interferometric signals can be obtained.

$$\tilde{c}_i = \frac{\int \mathrm{d}A E_1 E_2^* \tilde{R}_i}{\sqrt{\int \mathrm{d}A E_1 E_1^* \tilde{R}_i}\sqrt{\int \mathrm{d}A E_2 E_2^* \tilde{R}_i}}, \tag{1}$$

where A is the total area of the integral, E_1 and E_2 are the interfering electric fields, and $\tilde{R}_i$ is the weighting factor from the measured normalized spatial response of segment i. E_1, E_2, and $\tilde{R}_i$ are in general dependent on the x and y positions. For the standard IfoCAD QPD model, $\tilde{R}_i$ is equal to 1. The denominator contains the normalization factors. The result $\tilde{c}_i$ is the normalized complex amplitude of segment i. To allow the adaptive integration method to evaluate the electric fields in any given point of the integral surface A, the $\tilde{R}_i$ values needed are calculated using bilinear interpolation, with the response matrix as input. Once the electric fields are integrated over the QPD surface, IfoCAD can easily provide the fundamental measurands of the interferometric system. The normalized complex amplitudes are used to obtain the longitudinal path length signal (LPS) and the DWS signals (expressions (2)–(4))

$$\mathrm{LPS} = \frac{\lambda}{2\pi}\arg(\tilde{c}_A + \tilde{c}_B + \tilde{c}_C + \tilde{c}_D)\ [\mathrm{m}], \tag{2}$$

$$\mathrm{DWS}_H = \arg\left(\frac{\tilde{c}_A + \tilde{c}_C}{\tilde{c}_B + \tilde{c}_D}\right)\ [\mathrm{rad}], \tag{3}$$

$$\mathrm{DWS}_V = \arg\left(\frac{\tilde{c}_A + \tilde{c}_B}{\tilde{c}_C + \tilde{c}_D}\right)\ [\mathrm{rad}]. \tag{4}$$

Here λ is the wavelength of the light wave. Figure 5 shows a block diagram of the process. Comparing the results of using the standard QPD model versus the measured QPD response, we can draw conclusions about the effect of the QPD spatial response features on the measurands.

5. SIMULATION SETUP AND RESULTS

Since the main motivation of this work was to study the influence of nonuniform responses on the main measurands, the

QP22 QPD response was chosen for the simulations in IfoCAD. The larger fluctuations in the QP22's response would in principle intensify degradations in the performance. In general, imaging systems are used in laser interferometers to focus beams on the photodiode surface, reduce beam walk that could produce unwanted tilt-to-length coupling, and remove diffraction patterns in clipped top-hat beams. The lens system images the receive aperture and the local beam waist onto the QPD surface, as depicted on the left side of Fig. 6. In the particular case of the GRACE-FO mission, both input beams have the same angle of incidence, which varies a few millirad during operation due to spacecraft altitude changes.

The pivot point for tilts in the input beams would ideally be located on the photodiode center itself. Positioning errors (P_e) when building the optical bench could translate to a slightly off-photodiode position, which leads to beam walk and tilt-to-length coupling. In the simulations, we applied variations to the input angle to understand the coupling in the main longitudinal and DWS signals in the presence of photodiode placement deviations. We first used the standard IfoCAD QPD model with a 2.7 mm radius and a 70 μm gap width (according to the QP22 datasheet), and then the QP22 measured response. Three values for the separation between the pivot point and the photodiode (P_e) were used: 0, 0.5, and 1 mm. A 1.675-mm-waist radius Gaussian beam was used for the local beam, with the waist located at the pivot point. For the received beam, a top-hat beam larger than the QPD was used. This setup recreates the conditions of an intersatellite interferometric system like the one in GRACE-FO or eLISA.

The yaw and pitch tilts were applied to both beams simultaneously, which ideally would lead to zero longitudinal and DWS signals. The maximum absolute tilt used was 10 mrad.

Figure 7 shows the results obtained for the horizontal DWS signals. Results for the vertical DWS signal using different pitch tilts are equivalent and are omitted for the sake of clarity. There is a degradation toward larger P_e, where the DWS signals deviate from zero when tilts are applied. This occurs for both the standard and the measured QPD. Results indicate that the deviation slightly decreases with the measured QP22 response. In order to investigate this further, two additional simulations were performed using modified measured QPD responses. Figure 8 shows the single segment response used in these additional simulations (Cases 2 and 3), together with the standard QPD model (Case 1) and the unmodified measured QPD response (Case 4).

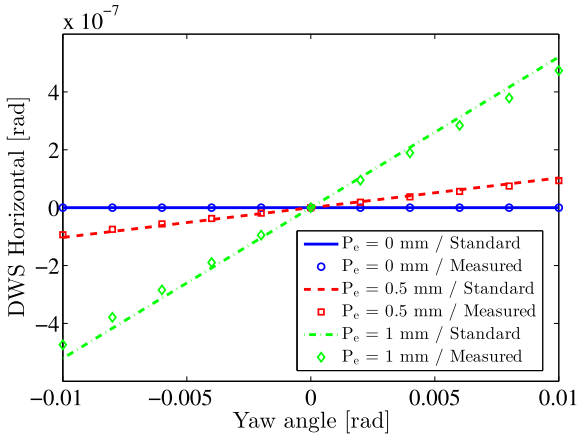

Fig. 7. Horizontal DWS signal for yaw tilts obtained in the simulations. Results for the vertical DWS signal using different pitch tilts are equivalent and are omitted for the sake of clarity. The tilt is applied to both beams simultaneously. Simulations were performed using three different distances between the pivot point and the photodiode (P_e), represented by different colors. The lines correspond to simulations with the standard IfoCAD QPD, and the markers to ones with the measured QP22 response.

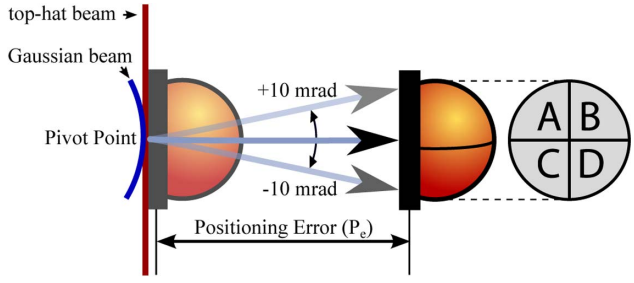

Fig. 6. Scheme of the simulation setup used, based on the interferometer conditions in an intersatellite laser ranging mission like GRACE-FO. A 1.675-mm-waist radius Gaussian beam (in blue) was used for the local beam with the waist located at the pivot point. The red line represents the received top-hat beam. Yaw and pitch tilts from −10 to 10 mrad were applied to both beams simultaneously, which would ideally lead to zero longitudinal and DWS signals. Three different QPD positions with respect to the pivot point (P_e) were used: 0, 0.5, and 1 mm, in order to study deviations from the ideal case.

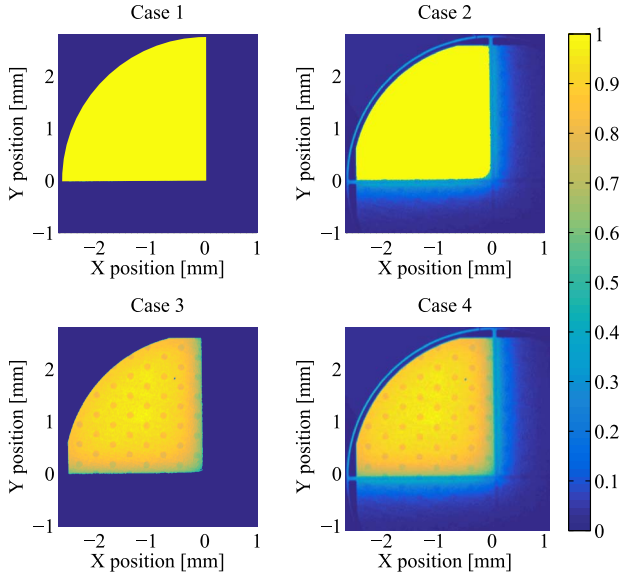

Fig. 8. Example of a single segment response of the standard QPD model (Case 1), the modified profiles for additional simulations (Cases 2 and 3), and the unmodified measured QPD response (Case 4). In Case 2, the QPD response is uniform within the segment and nonzero outside. That includes not only the gap but also the crosstalk from adjacent segments. Case 3 is the opposite: the response is nonuniform within the segment but zero outside.

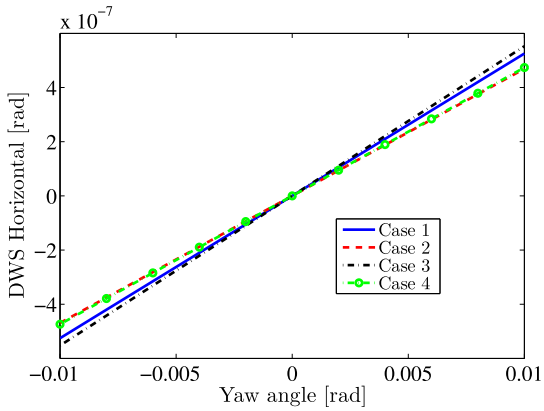

Fig. 9. Horizontal DWS signal for yaw tilts at $P_e = 1$ mm for all four cases of Fig. 8. Results for the vertical DWS signal are equivalent and are omitted for the sake of clarity.

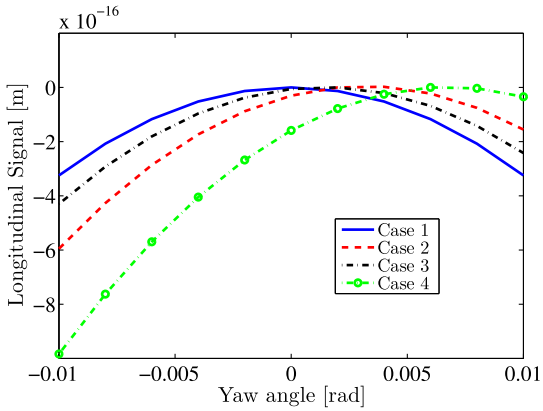

Fig. 11. Main longitudinal signal for yaw tilts at $P_e = 1$ mm for all four cases of Fig. 8. Results for tilts in pitch are equivalent and are omitted for the sake of clarity.

In Case 2, the QPD response is uniform within the segment and nonzero outside that includes not only the gap but also crosstalk from adjacent segments. Case 3 is the opposite: the response is nonuniform within the segment but zero outside. Figure 9 shows the results obtained for the horizontal DWS signals at $P_e = 1$ mm for all four cases. Again, results for the vertical DWS signal are equivalent and therefore omitted. Cases 2 and 4 present roughly the same deviation, whereas it increases in Cases 1 and 3. These results indicate that a nonzero response in the gap and the presence of crosstalk decrease deviations from zero in the DWS signal independently of the uniformity within the segment. In all cases, the maximum deviation of $\sim 10^{-7}$ rad observed in the DWS signal is orders of magnitude below the maximum allowed value of 10^{-2} rad for GRACE-FO.

Figure 10 shows the effect of simultaneous yaw tilts in both beams on the main longitudinal signal. Results for tilts in pitch are equivalent and therefore omitted. Once again, we can see a degradation toward larger P_e for both the standard and the measured QPD since the main longitudinal signal deviates from zero in a quadratic fashion when tilts are applied. The maximum of this quadratic trend shifts from 0 mrad to larger angles when the measured QPD response is used. Additional simulations at $P_e = 1$ mm were performed using the modified QPD responses of Fig. 8. Results are shown in Fig. 11. We can verify the shift of the maximum for different responses. This maximum represents also the point of minimum coupling of this quadratic relation between the tilt angle and the longitudinal signal. In all cases, the maximum deviation of $\sim 10^{-15}$ m is very low compared to the maximum allowed value of 10^{-6} m for GRACE-FO.

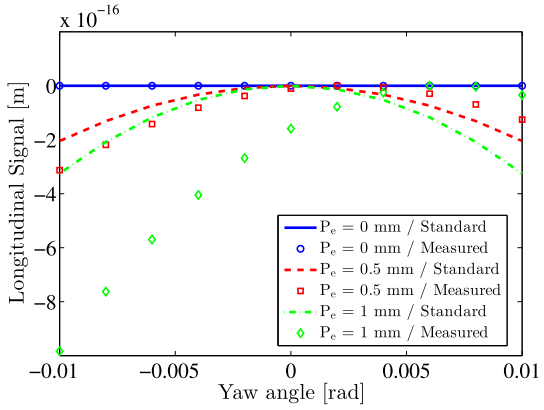

Fig. 10. Main longitudinal signal for yaw tilts obtained in the simulations. Results for tilts in pitch are equivalent and are omitted for the sake of clarity. The tilt is applied to both beams simultaneously. Simulations were performed using three different distances between the pivot point and the photodiode (P_e), represented by different colors. The lines correspond to simulations with the standard IfoCAD QPD, and the markers correspond to ones with the measured QP22 response.

6. CONCLUSIONS

The effect of a real photodiode response on the main longitudinal and DWS signals of a laser interferometer was studied. First, we have presented a setup to perform spatially resolved scans of QPDs. The presented setup achieves a spatial resolution of 50 μm, which is limited by the laser spot diameter. We have measured the spatial response of three different QPD candidates for space interferometry using this setup. Results from the QP22 present a nonuniform profile with a distribution of 20% reduced responsivity spots. The spatial response of the FCIQ1000 and GAP9119 appear uniform with maximum responsivity deviations around 1% within the active area. We have developed an extension for the IfoCAD simulation software, which allows us to use the measured response of a QPD in our simulations. The specific case studied features a local Gaussian beam and a received top-hat beam, a maximum QPD positioning error of 1 mm, and a maximum absolute tilt of 10 mrad. The simulations were performed with both the standard IfoCAD QPD model and the measured response of the QP22. Results from these simulations indicate that deviations in the main measurands are of no concern for the specific case studied, including standard and measured QPD profiles. This could open the door to future photodiode candidates that have excellent characteristics, such as a very

low junction capacitance, and would otherwise have been rejected due to a nonstandard profile.

The scans could be improved by reducing the spot size of the beam. The measured responses presented here are a convolution of the probing 50 μm Gaussian beam with the actual QPD response. Numerical deconvolution was tested as an alternative to beam reduction, but it introduces unwanted disturbances. In the simulation environment, the large top-hat beam could be replaced with a more realistic clipped beam, whose diffraction patterns might also influence the measurands of interest.

Funding. Max-Planck-Institut für Gravitationsphysik (Institut für Gravitationsphysik, Leibniz Universität Hannover).

REFERENCES

1. B. Sheard, G. Heinzel, K. Danzmann, D. Shaddock, W. Klipstein, and W. Folkner, "Intersatellite laser ranging instrument for the GRACE follow-on mission," J. Geod. **86**, 1083–1095 (2012).
2. E. Morrison, B. J. Meers, D. I. Robertson, and H. Ward, "Experimental demonstration of an automatic alignment system for optical interferometers," Appl. Opt. **33**, 5037–5040 (1994).
3. E. Morrison, B. J. Meers, D. I. Robertson, and H. Ward, "Automatic alignment of optical interferometers," Appl. Opt. **33**, 5041–5049 (1994).
4. H. Gong, L. Hanssen, and G. Eppeldauer, "Spatial and angular responsivity measurements of photoconductive HgCdTe LWIR radiometers," Metrologia **41**, 161–166 (2004).
5. M. Durak, "Spatial non-uniformity analyses of radiometric detectors to identify suited transfer standards for optical radiometry," Eur. Phys. J. **32**, 193–197 (2005).
6. A. Lamminpaa, M. Noorma, T. Hyyppa, F. Manoocheri, P. Karha, and E. Ikonen, "Characterization of germanium photodiodes and trap detector," Meas. Sci. Technol. **17**, 908–912 (2006).
7. F. Seifert, "Power stabilization of high power laser for second generation gravitational wave detectors," Ph.D. thesis (Leibniz Universität Hannover, 2010).
8. N. Fox, E. Theocharous, and T. Ward, "Establishing a new ultraviolet and near-infrared spectral responsivity scale," Metrologia **35**, 535–541 (1998).
9. A. Corrons, J. Fontecha, P. Corredera, J. Campos, A. Pons, and M. Hernanz, "Ultraviolet calibration of detectors with respect to a cryogenic radiometer," Metrologia **37**, 555–558 (2000).
10. M. Durak, F. Samadov, and A. Turkoglu, "Spatial non-uniformity measurements of large area silicon photodiodes," Turk. J. Phys. **26**, 375–380 (2002).
11. L. C. Alves, F. Reis, M. C. Torres, G. B. Almeida, and I. B. Couceiro, "Spatial uniformity of the silicon photodiodes for establishment of spectral responsivity scale," in *Proceedings of XIX IMEKO World Congress: Fundamental and Applied Metrology* (IMEKO, 2009), pp. 164–167.
12. A. Makynen and J. Kostaniovaara, "Electro-optical instrument for photodetector characterization," in *Proceedings of IEEE Conference on Instrumentation and Measurement Technology* (IEEE, 2004), Vol. **3**, pp. 2365–2368.
13. E. Theocharous, M. A. Itzler, J. Cheung, and C. J. Chunnilall, "Characterization of the linearity of response and spatial uniformity of response of two InGaAsP/InP Geiger-mode avalanche photodiodes," IEEE J. Quantum Electron. **46**, 1561–1567 (2010).
14. G. Wanner, G. Heinzel, E. Kochkina, C. Mahrdt, B. Sheard, S. Schuster, and K. Danzmann, "Methods for simulating the readout of lengths and angles in laser interferometers with Gaussian beams," Opt. Commun. **285**, 4831–4839 (2012).
15. J. A. Arnaud, W. M. Hubbard, G. D. Mandeville, B. de la Clavière, E. A. Franke, and J. M. Franke, "Technique for fast measurement of Gaussian laser beam parameters," Appl. Opt. **10**, 2775–2776 (1971).
16. F. Blumenschein, "Spatially resolved characterization of RF QPDs," Bachelor's thesis (University of Konstanz, 2011).